BIOCHIP JOURNAL, Vol. 1, No. 4, 234-240, December 2007

Optoelectronic Manipulation of Microparticles Using Double Photoconductive Layers on a Liquid Crystal Display

Hyundoo Hwang[1], Youngjae Oh[1], Jae-Jun Kim[1], Wonjae Choi[1], Se-Hwan Kim[2], Jin Jang[2] & Je-Kyun Park[1]

[1]Department of Bio and Brain Engineering,
Korea Advanced Institute of Science and Technology (KAIST),
335 Gwahangno, Yuseong-gu, Daejeon 305-701, Korea
[2]Department of Information Display, Kyung Hee University,
1 Hoegi-dong, Dongdaemun-gu, Seoul 130-701, Korea
Correspondence and requests for materials should be addressed to J.-K. Park (jekyun@kaist.ac.kr)

Accepted 18 September 2007

Abstract

This paper describes a novel platform for the optoelectronic manipulation of microparticles termed a three-dimensional optoelectronic tweezers (3D OET) and composed of double photoconductive layers. The 3D OET has been successfully utilized for focusing polystyrene beads onto the middle of a liquid chamber using negative dielectrophoresis (DEP). As a result, the microparticles are segregated from the device surface, thus preventing the adsorption by non-specific surface-particle interactions which were shown to occur in a typical OET device. We have compared the performance of 3D OET to typical OET based on a liquid crystal display (LCD) with several parameters, such as LCD image patterns, bead sizes and processing times. The 3D OET has a higher particle trapping efficiency and less particle adsorption rate than typical OET. Our novel platform would be a useful tool for manipulating microparticles, including live cells and polymer beads.

Keywords: Dielectrophoresis, Optoelectronic tweezers, Liquid crystal display (LCD), Microfluidics

Introduction

Manipulation technologies, such as the transport, trapping and sorting of microparticles, as well as live cells, are essential for performing several biological and chemical applications, such as bead-based chemical analyses, single cell-based analyses, cell patterning, cell cultures and diagnostics in various clinical fields. For these purposes, several mechanisms, including optical[1], magnetic[2], electrokinetic[3], acoustic[4] and hydrodynamic[5] forces have been applied. Among these principles, dielectrophoresis (DEP) is the most favorable tool for microparticle manipulation since the modification of a target particle is not required and the construction of a patterned electrode array for the parallel manipulation with lower power consumption and larger manipulation area is possible[6-8]. Recently, a novel principle termed optoelectronic tweezers (OET) or light-induced DEP has been proposed by Chiou *et al.*[9]. The principle describes the replacement of patterned electrodes with a pattern-less photoconductive layer. As a result, the light-induced virtual electrodes are formed on the photoconductive layer by projecting a dynamic image generated from a digital micro-mirror device (DMD). Since the OET requires lower optical power and offers higher massiveness than typical optical tweezers, it has become a powerful technology for the parallel manipulation of microparticles, which includes biological cells[10]. Previously, we reported a novel OET platform termed lab-on-a-display, to supply the need for simple and portable OET system[11]. The lab-on-a-display is constructed with an OET device and a liquid crystal display (LCD) without additional optical components. As a result, the lab-on-a-display provides a more suitable platform for portable applications.

In typical OET device, unidirectional vertical forces as well as lateral forces act on the particles. The vertical forces provide an upward force on the particles when a negative DEP is induced. Consequently, the manipulated particles are positioned at the upper region of the liquid layer and frequently become attached to the top ground layer by non-specific interactions between the particles and the surface of the device. The non-specific interactions, including hydrophobic and electrostatic surface-particle interactions, interfere with the effective and non-contact particle manipulations within the scheme of OET. In addition, some attached particles attract other nearby particles around them by electrostatic particle-particle attractions[12,13], thus limiting their smooth movements and their stable long-term processes. Some relatively small particles are sometimes put out of focus because of their vertical movements, resulting in a low particle trapping efficiency. These problems are magnified when the microparticles require free handling in the channel-less environments like the OET. Additionally

in the case of biological samples which can easily be contaminated or damaged by an external stimulus, the interactions with device surfaces may exert fatal influences on them. Nevertheless, the particle-surface interactions are unavoidable for a conventional OET device, in which the vertical DEP forces, which act on only one direction by negative or positive DEP, are uncontrollable.

In order to deal with these problems in a typical OET device, we need to focus the manipulated particles vertically to keep them apart from the surfaces of the OET device, which means that the three-dimensional trapping of particles, such as optical tweezers, are required. Therefore, we suggest a novel OET platform termed three-dimensional optoelectronic tweezers (3D OET), which are composed of double photoconductive layers. In the 3D OET device, the liquid layer containing microparticles is sandwiched between two photoconductive layers (Figure 1B) in a different manner than the OET device composed of photoconductive and ground layers (Figure 1A). When an AC bias voltage is applied between two photoconductive layers, the transmitted light beam forms virtual electrodes on the surfaces of the top and the bottom photoconductive layers, which result in an electric field gradient in the liquid. This electric field gradient generates dipole moments in neutral particles and cause DEP forces for microparticle manipulation. The virtual electrodes in the 3D OET generate 3D DEP cages which trap the particles and focus them vertically. Consequently, the vertical focusing and 3D trapping of the microparticles, using a 3D OET device, allows the possibility of adsorption-free particle manipulation.

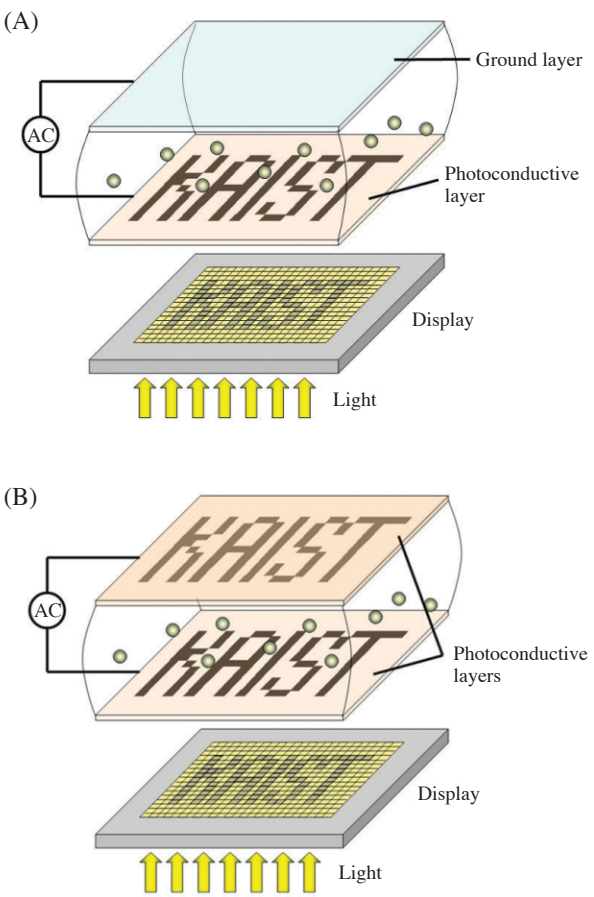

Figure 1. Schematic diagrams of (A) optoelectronic tweezers (OET) and (B) three-dimensional optoelectronic tweezers (3D OET). The 3D OET device is composed of two photoconductive layers, while the OET device is composed of one photoconductive layer and a ground layer.

Results and Discussion

Simulated Electric Field Distribution

The electric field distribution in the liquid chamber of 3D OET was simulated and described in comparison to typical OET (Figure 2). The electric field was calculated using a commercial CFD solver (CFD-ACE+; ESI US R & D Inc., Huntsville, AL, USA). We assumed the application of a 10 V bias at 100 kHz,

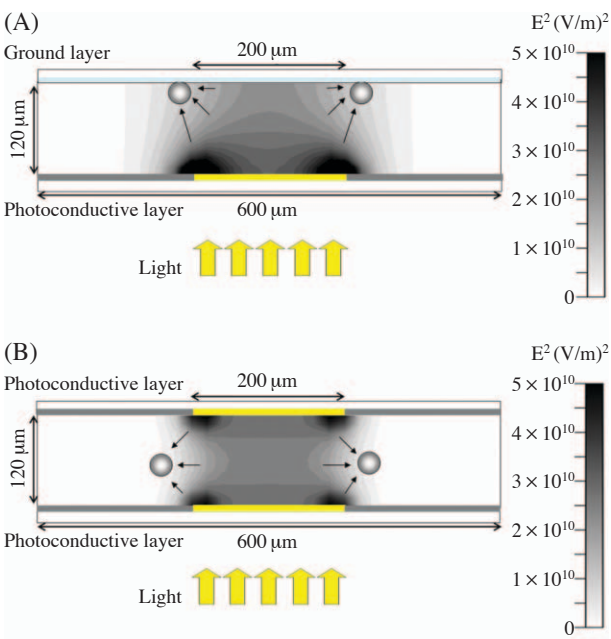

Figure 2. Simulated electric distributions in the liquid chamber of (A) OET and (B) 3D OET with an estimate of particle movements. In the OET device, the microparticles would be moved upward and adsorbed at the surface of the ground layer following a negative DEP. For 3D OET, the microparticles would be focused onto the middle of the liquid chamber and segregated from the surface of the top layer.

to the illuminated area of the bottom photoconductive layer of both devices. In the OET device, all areas of the top ground layer were assumed to be a ground. In contrast, for the 3D OET device, only the illuminated area of the top photoconductive layer, which is the same as the bottom photoconductive layer, was assumed to be a ground. We could find the electric field differences between OET and 3D OET through the simulation study.

According to the simulation results, the microparticles following negative DEP would move in the direction of the dark region (which has a strong electric field region) to the light region (which has a weak electric field region). That is, the microparticles in the 3D OET device would be focused onto the middle of the liquid layer and segregated from the surface of the device (Figure 2B). Consequently, we can manipulate the target particles free from any surface-particle interactions, when using the 3D OET device. In addition, since the DEP force acting on a particle is proportional to the gradient of the square of the electric field, the focused particles in 3D OET can move faster than those in typical OET.

Vertical Focusing of Microbeads

Microscopic images at three different heights-bottom, middle and top- of the liquid chamber are shown in Figure 3. In the 3D OET device, the polystyrene beads were successfully focused onto the middle of the liquid layer (Figure 3B), while adsorbed on the surface of the top ground electrode by electrostatic surface-particle interactions in the OET device (Figure 3A).

Increased Trapping Efficiency

We measured the particle trapping efficiency in the OET and 3D OET devices by counting the number of moving particles in both devices under the experimental condition, at which the attached particles are not moved. Figure 4A shows the percentage of moving particles by several LCD images in the OET and 3D OET devices. The images appear gradually during 60 s, forming the letters “I”, “X” and “O”. We assumed that the microparticles were uniformly spread out at the initial state, to allow the calculation of the percentage of particles moved by those images over the total number of particles. The percentage of particles successfully moved by 3D OET was about twice as much as in typical OET. Moreover, the microscopic photographs of the concentrated particles by LCD images which formed the letter “O” (the inside of dotted lines is dark region) in the OET and 3D OET devices are shown in Figure 4B. The particle trapping efficiency by DEP forces was significantly increased

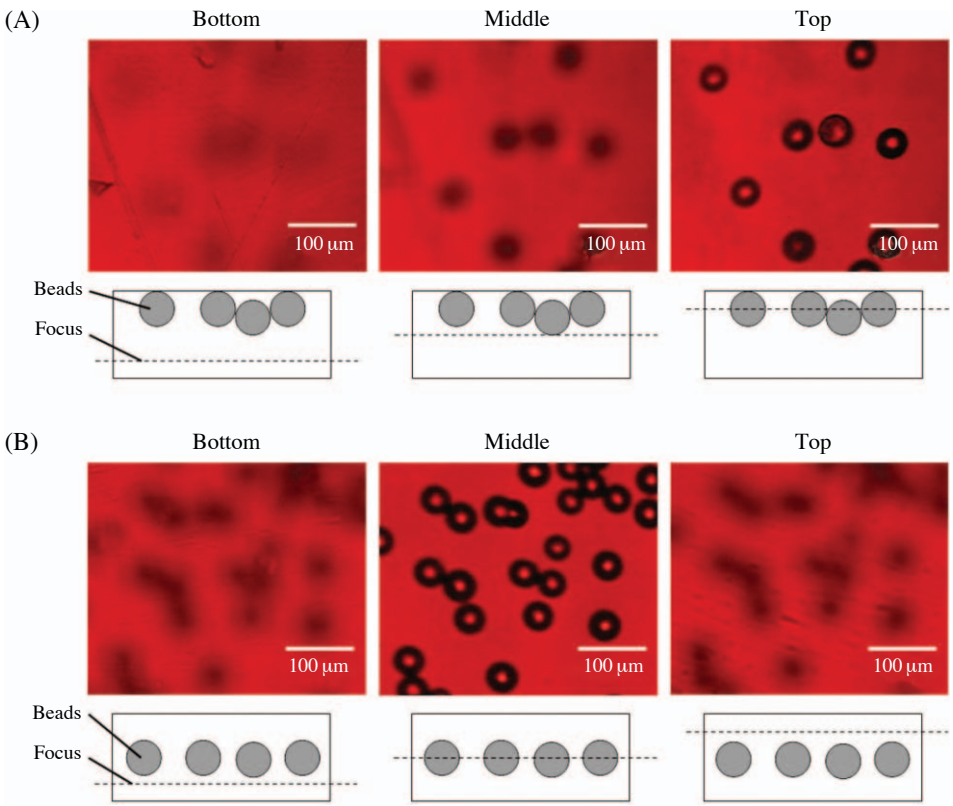

Figure 3. Microscopic photographs as a function of the heights of the liquid layers of the (A) OET and (B) 3D OET devices. The schematic diagrams of cross-sections are also represented. In the 3D OET device, the polystyrene beads (45 μm diameter) were focused onto the middle of the liquid layer, while being adsorbed on the surface of the ground layer by negative DEP in the OET device.

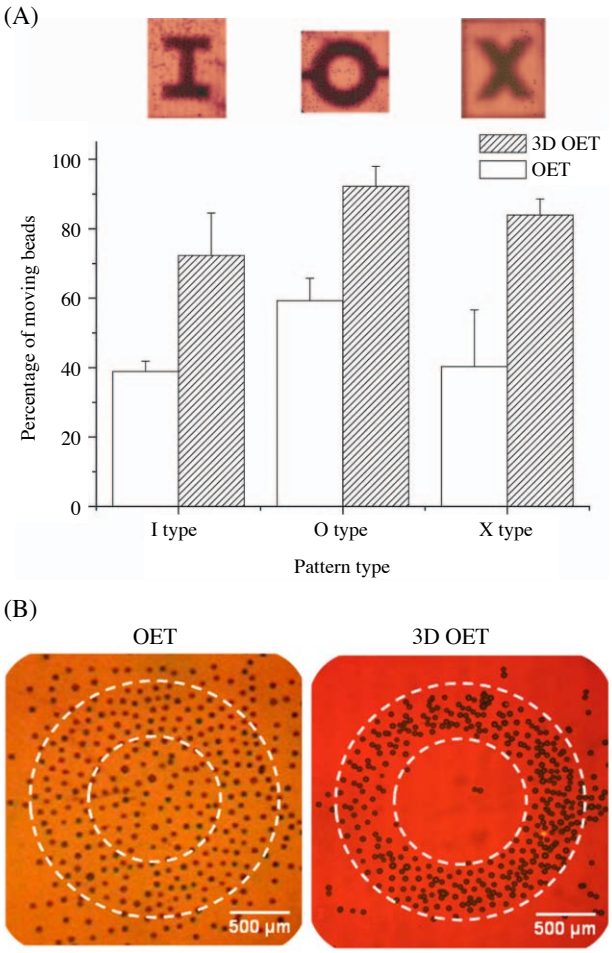

Figure 4. (A) The percentage of moving beads by several LCD images in the OET and 3D OET devices (mean ± standard deviation, n ≥ 5). The images appear gradually over 60 s, forming the letters "I", "X" and "O". (B) The microscopic photographs of the polystyrene beads (45 μm diameter) were concentrated by the OET and 3D OET devices. An LCD image appeared gradually over 60 s, and formed letter "O". The microbeads should have been moved to the inside of the dotted line.

in the 3D OET.

Effect of Bead Size

The percentage of moving particles according to the particle size in the OET and 3D OET devices is shown in Figure 5. While less than 50% of particles could be moved without adsorption in OET devices, only a few particles were adsorbed in 3D OET devices. We could more clearly delineate the superior performance of the 3D OET by comparing the percentage of displaced 90 μm diameter particles in a 120 μm gap height liquid chamber. The adsorption of microparticles by surface-particle interactions be-

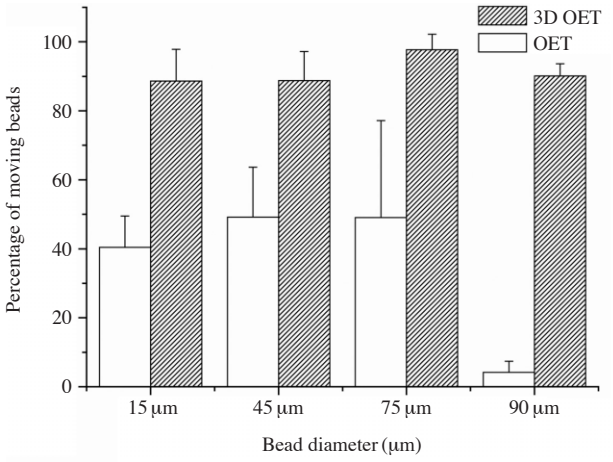

Figure 5. The percentage of moving beads according to bead size in the OET and 3D OET devices (mean ± standard deviation, n ≥ 5). The gap height in the liquid chamber was 120 μm and a 20 V bias at 100 kHz was applied.

comes more apparent when we manipulate relatively larger beads. For 3D OET, we could manipulate most of the 90 μm diameter beads, despite their relatively larger size. In contrast, more than 90% of the microbeads were adsorbed onto the surface of the upper ground electrode and failed to be successfully manipulated in the OET device.

Time Domain Analysis

To investigate the time-dependant phenomenon of particle adsorption in the OET device, compared to the 3D OET device, we measured the percentage of moving beads in each device over a specific period of time. The result of the time domain analysis is described in Figure 6. While the percentage of moving beads in the OET device decreases with time, most of the particles in the 3D OET device were continuously moved without attachments. The attached particles in the OET induced strong electrostatic attractive forces which drew other particles around them, and thus interferes with the continuous particle manipulation over the long term. This became a serious issue when a long-term particle manipulation was required. We can solve the problem by using the 3D OET which can continuously prevent the particle-particle aggregations as well as the particle-surface interactions.

Conclusions

In this paper, a 3D OET made up of two photoconductive layers as a pair, for 3D trapping and manipulation of microparticles has been developed. We have

successfully manipulated polystyrene beads without attachment using 3D OET on a LCD. The performance of the 3D OET was compared with OET for several parameters including: 1) LCD image, 2) bead size and 3) manipulation time. For the 3D OET device, about 90% of target particles were successfully manipulated on continuous basis for a relatively long period of time ($t \geq 450$ s), while about 50% of particles were adsorbed onto the surface of the device or focused out by vertical forces in the OET device. In the case of the 90 μm diameter beads in the 120 μm liquid layer gap height, about 95% of the beads were adsorbed onto the device surface of the OET. In contrast, we could successfully demonstrate the adsorption-free particle manipulation using 3D OET regardless of the particle size and the height of liquid layer. The higher trapping efficiency and adsorption-free particle manipulation resulted in the 3D OET platform to be a more compatible tool for the microparticle manipulation in medical and biological applications.

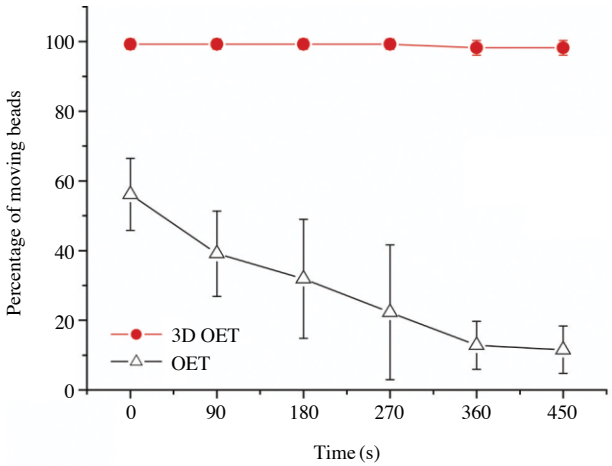

Figure 6. The percentage of moving beads according to time in the OET and 3D OET devices (mean ± standard deviation, $n \geq 5$). While the number of moving beads in OET decreases with time, most of the particles in the 3D OET device were moved continuously without adsorption.

Materials and Methods

Device Fabrication

We used an indium tin oxide (ITO) layer for the transparent and conductive layer in the ground layer of the OET device. Both of the photoconductive layers

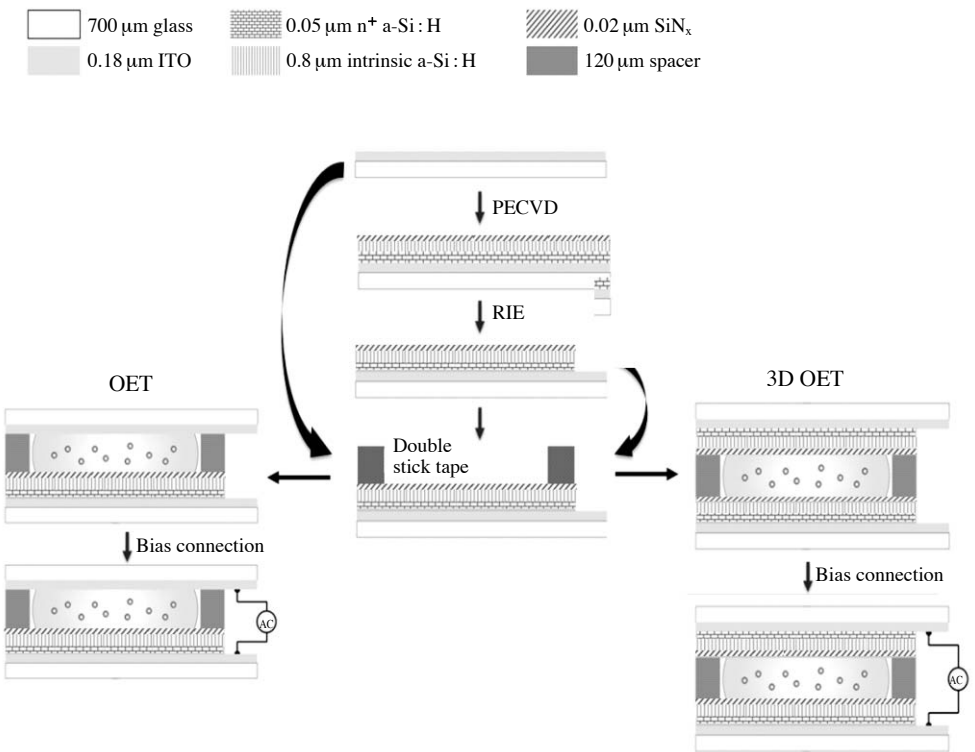

Figure 7. Fabrication processes of the OET (left) and 3D OET devices (right). The fabrication processes for the photoconductive layers of each device were identical. For the 3D OET, the liquid layer containing microparticles is sandwiched between two photoconductive layers.

in the OET and 3D OET devices were comprised of four layers: 1) a 180 nm thick ITO layer, 2) a 50 nm thick n^+ doped hydrogenated amorphous silicon (n^+ a-Si : H) layer, 3) a 800 nm thick intrinsic hydrogenated amorphous silicon (intrinsic a-Si : H) layer, and 4) a 20 nm thick silicon nitride (SiN_x) layer. In this study, the ITO-coated glass substrates (Samsung-Corning Precision Glass, Asan, Korea) were used to fabricate the photoconductive layers of our devices. Furthermore, a triple layer of n^+ a-Si : H, intrinsic a-Si : H and SiN_x was consecutively deposited by plasma enhanced chemical vapor deposition (PECVD) onto the substrate. Next, some regions were etched for bias connections by a reactive ion etch (RIE) to expose the ITO layer. After dicing the fabricated device into 37.5 mm × 25.0 mm sections, a wrapping wire was connected for biasing. Finally, we turned one photoconductive layer upside down and placed it on the top of the other photoconductive layer at the regular gap space using double-stick tape as a spacer. While utilizing the OET device, the ITO ground layer was replaced in the upper photoconductive layer of the 3D OET device. The fabrication processes of each device are shown in Figure 7.

Experimental Setup and Analysis

To operate the OET and 3D OET devices, a 1.3 inch monochromatic LCD module was used[11], consisting of a 800 × 600 pixel array with a 33 μm pixel pitch. A standard presentation software program (Microsoft PowerPoint™) and an interactive control program (which we developed) was utilized for the automatic image pattern formations in Figures 4 and 5, and the long-term pattern manipulation in Figure 6, respectively.

Plain polystyrene beads (PolySciences, PA, USA) were used for the particle manipulation in the 20 V bias condition at 100 kHz. The sample was prepared by diluting de-ionized water (conductivity-0.23 mS/m). A sample droplet was sandwiched between two photoconductive layers (or a photoconductive and a ground layer) using 120 μm thick double-stick tape as a spacer. Next, the bias voltage, which was produced from a function generator (AGF3022: Tektronix, USA) was applied.

Two illuminations of the microscope were used: one for actuation and the other for observation. The downside illumination (with high intensity) was used for actuation, (i.e. to create the image for virtual electrodes) whereas, the upside illumination (with low intensity) was used for observation since it was difficult to see the particles in a dark region without the upside illumination. To measure the bead velocities, we recorded the bead movements and analyzed the video files with an analysis program which we developed using MATLAB. The microscopic pictures, except for Figure 4A, were taken without any image patterns of LCD, because the optical observation of the beads in the dark region was limited for the 3D OET device. Furthermore, to observe and capture the displaced particles in the dark region, we brightened the whole LCD area with a full white screen after all manipulation processes were completed.

Acknowledgements

This research was supported by the Nano/Bio Science & Technology Program (2006-00955) of the Ministry of Science and Technology (MOST), Korea. The authors also thank the CHUNG Moon Soul Center for BioInformation and BioElectronics, KAIST. The microfabrication work was performed at the TFT -LCD Research Center (Kyung Hee University, Seoul, Korea).

References

1. Grier, D.G. A revolution in optical manipulation. *Nature* **424**, 810-816 (2003).
2. Lee, H., Purdon, A.M. & Wetervelt, R.M. Manipulation of biological cells using a microelectromagnet matrix. *Applied Physics Letter* **85**, 1063 (2004).
3. Green, N.G., Ramos, A. & Morgan, H. AC electrokinetics: a survey of sub-micrometre particle dynamics. *Journal of Physics D Applied Physics* **33**, 632-641 (2000).
4. Hertz, H.M. Standing-wave acoustic trap for nonintrusive positioning of microparticles. *Journal of Applied Physics* **78**, 4845-4849 (1995).
5. Fu, A.Y. *et al.* A microfabricated fluorescence-activated cell sorter. *Nature Biotechnology* **17**, 1109-1111 (1999).
6. Pohl, H. *Dielectrophoresis*, Cambridge University Press: 1978.
7. Choi, S. & Park, J.-K. Microfluidic system for dielectrophoretic separation based on a trapezoidal electrode array. *Lab on a Chip* **5**, 1161-1167 (2005).
8. Manaresi, N. *et al.* A CMOS chip for individual cell manipulation and detection. *IEEE Journal of Solid-State Circuit* **38**, 2297- 2305 (2003).
9. Chiou, P.Y., Ohta, A.T. & Wu, M.C. Massively parallel manipulation of single cells and microparticles using optical images. *Nature* **436**, 370-372 (2005).
10. Ohta, A.T. *et al.* Optically controlled cell discrimination and trapping using optoelectronic tweezers. *IEEE Journal of Selected Topics in Quantum Electronics* **13**, 235-243 (2007).
11. Choi, W., Kim, S.-H., Jang, J. & Park, J.-K. Lab-on-

a-display: a new microparticle manipulation platform using a liquid crystal display (LCD). *Microfluidics and Nanofluidics* **3**, 217-225 (2007).
12. Kang, K.-H. & Li, D. Dielectric force and relative motion between two spherical particles in electrophoresis. *Langmuir* **22**, 1602-1608 (2006).
13. Velev, O.D. & Bhatt, K.H. On-chip micromanipulation and assembly of colloidal particles by electric fields. *Soft Matter* **2**, 738-750 (2006).